A Development of Gold Nanodots Fabrication for Optical Plasmonic Applications

Thitipoom Dorkyor[1], Potejana Potejanasak[2*], Chamaporn Chianrabutra[1], Chana Raksiri[3]

[1]Department of Mechanical Engineering, Faculty of Engineering, Kasetsart University, Bangkok, Thailand
[2]Department of Industrial Engineering, School of Engineering, University of Phayao, Phayao, Thailand
[3]Department of Industrial Engineering, Faculty of Engineering, Kasetsart University, Bangkok, Thailand

Optical plasmonic sensing is an up-and-coming technique for label-free biosensing, particularly in detecting antigen-antibody binding. This research introduces an efficient nanofabrication method, employing the self-organization approach of thermal annealing to create gold nanodots on a quartz substrate. Fabrication involved careful sputter depositing and thermal annealing procedures to achieve optimal results. A 24 full-factorial design was implemented to assess the average diameter of gold nanodots. The investigation focused on evaluating the impact of varying parameters, including the thickness of the gold film on the quartz substrate, annealing temperature, annealing time, and chemical treatment applied to the surface of the quartz substrate. Statistical analysis considering the main effects and mixed interactions between factors revealed that the chemical treatment on the quartz substrate's surface emerged as the most influential parameter in determining the gold nanodot characteristics. Significantly, the results underscored an optimum thermal annealing condition for gold nanodot aggregation, characterized by a thickness of the gold film of 30 nm, annealing temperature of 700°C, and annealing time of 30 minutes, along with surface treatment on the quartz substrate. Validated at a significant level of 95%, these findings provide valuable insights for refining and optimizing the nanofabrication process, contributing to advancing plasmonic biosensing applications.

Keywords: Gold nanodot fabrication, Design of experiment, Thermal annealing, Plasmonic Biosensing.

1. Introduction

The field of optical plasmonic sensing has risen to prominence as a highly acclaimed biosensor, finding widespread applications in diverse domains such as medical, agricultural, and food-related fields. This innovative technology facilitates the detection of a broad spectrum of biomolecules, including enzymes, proteins, and viruses [1-3]. This biosensor's core lies in a critical component, an intricately designed nanometer-scale, high-purity metal structure on quartz substrates. Gold nanodots provide numerous benefits for optical plasmonic sensing. They are characterized by their solid plasmonic properties, which facilitate highly sensitive detection of molecular interactions. Their adaptable plasmonic resonance allows customization for specific sensing applications. Gold's biocompatibility also ensures that nanodots are suitable for biological sensing without cytotoxic effects. By functionalizing with various biomolecules, nanodots enable selective detection and multiplexed sensing. Furthermore, label-free detection streamlines assay protocols, reducing costs. Nonetheless, challenges exist; intense light exposure may lead to photobleaching, diminishing signal intensity and sensitivity. Spectral overlap or cross-reactivity issues might constrain multiplexing capabilities, and background signals from nonspecific interactions or the surrounding environment may interfere with detection specificity and sensitivity, necessitating careful optimization strategies. Despite these drawbacks, gold nanodots remain promising for advancing optical plasmonic sensing, owing to their versatile capabilities and potential applications. The efficacy of optical plasmonic sensing is intricately linked to the fabrication method employed for this nanostructure. Therefore, the refinement and optimization of the fabrication process have become paramount, exerting a pivotal influence on this biosensing technology's overall capabilities and effectiveness across a myriad of applications [4-7]. As research in biosensing continually evolves, advancements in the fabrication techniques for nanometer-scale metal structures contribute significantly to enhancing the precision, sensitivity, and versatility of optical plasmonic sensing, thereby expanding its potential impact in various scientific, medical, and industrial contexts.

In the conventional paradigm, the fabrication of gold structures on quartz substrates follows an approach employing ion beam focusing. Gallium ions (Ga+ Ion) are meticulously utilized to drill or extract small-scale objects at the nanometer level, inducing structural modifications in various materials [8-11]. However, this established technique confronts formidable production challenges. The process requires sluggish electron beam compression to penetrate diminutive gold sections, resulting in protracted fabrication times. The associated equipment is marked by prohibitive costs, contributing to financial constraints, and raises environmental concerns due to the deployment of hazardous chemicals. Alternative methods for fabricating gold structures on quartz substrates include electron beam lithography (EBL), which offers high resolution but is time-consuming, has limited scalability, and is expensive. Thermal evaporation deposits gold films quickly but lacks precision in structure formation and poor resolution. Chemical vapor deposition (CVD) allows for controlled growth but may require specialized equipment and complexity. This predicament prompts a compelling exploration for more cost-effective and environmentally sustainable alternatives in synthesizing gold structures on quartz substrates. The pursuit of

such alternatives aligns with the imperative to enhance the efficiency, accessibility, and eco-friendliness of gold structure fabrication methodologies, underscoring the continual evolution in the field of biosensing technologies.

Considering the challenges mentioned above, researchers globally are proactively delving into alternative nanoscale gold structure fabrication methodologies. This exploration places a premium on simplicity, convenience, rapidity, cost-effectiveness, and avoiding toxic chemicals. The impetus behind this burgeoning research initiative is a direct response to the escalating demand for medical biosensors, particularly in medical plasmonic biosensors like Lab-on-a-chip technologies. This research aims to elevate the efficiency of nanofabrication processes tailored for gold structures, thereby refining the precision in measuring and analyzing molecular types by harnessing their light absorption properties [12, 13]. This collaborative endeavor significantly contributes to the progression of biosensing technologies, which are pivotal in diverse medical applications. By focusing on innovative, eco-friendly, and accessible approaches to gold structure fabrication, this research addresses the pressing challenges associated with traditional methods, heralding a new era in biosensing methodologies with enhanced efficacy and applicability.

This study pioneers an innovative and rapid nanofabrication [14-17] approach for gold structures on quartz substrates, utilizing the Argon sputter coating process, which uses argon gas to dislodge material from a target onto a substrate to create the thin and uniform film [18, 19] and the self-organization method by a thermal annealing process [20-23] to fabricate the gold nanodot on a quartz substrate for plasmonic sensing is proposed. This process offers notable benefits for gold structure fabrication in plasmonic biosensors. It is cost-effective, requiring essential equipment with lower upfront costs than techniques like electron beam lithography or focused ion beam milling. It is environmentally friendly, uses less chemicals and waste than wet etching or photolithography, and is energy efficient. Moreover, it enhances material efficiency by controlling heating, reducing waste, and improving resource utilization. It is scalable for large-scale production and enables mass fabrication of biosensors without significant cost or environmental impact. In essence, the self-organization method by a thermal annealing process provides a cost-effective, eco-friendly approach, appealing to researchers and industries emphasizing performance, cost-effectiveness, and sustainability. This research was driven by the Design of Experiments (DOE) principles [24, 25], which aimed to optimize the fabrication processes to identify the most practical combination of process parameters that yield desired properties in nanodot arrays. These optimized parameters were subsequently applied to fabricate gold nanoparticle structures with heightened optical measurement properties. This unconventional methodology not only propelled advancements in the realm of nanofabrication but also underscored the effectiveness of the Design of Experiments (DOE) in fine-tuning and enhancing manufacturing processes, thereby elevating performance in optical sensing applications. By introducing this innovative approach, the study contributes to the evolution of biosensing technologies, offering a promising avenue for achieving precise and efficient fabrication of gold structures crucial for optical plasmonic sensing applications in diverse fields.

2. RESEARCH METHODOLOGY

This research was initiated with an exploration into the factors of the fabrication of the gold nanodot on quartz substrates and focused on discerning the critical contributors to achieving the minimum average diameter. Subsequently, the levels of these influential factors were meticulously determined, forming the basis for the gold nanodot fabrication process. These identified factor levels were then systematically integrated into the experimental design, leveraging the 2^k Full Factorial design method to explore the parameter space comprehensively.

This study's potential limitation is its reliance on gold nanodots for plasmonic biosensing applications. While gold nanodots have been extensively used in various sensing applications due to their unique optical properties, they also possess limitations that may affect their performance and practicality in specific contexts. However, the described nanofabrication method involving thermal annealing and chemical treatment requires precise control over multiple parameters to achieve reproducible results. Variability in fabrication conditions or substrate properties may affect the size, shape, and distribution of gold nanodots, thereby influencing the sensing performance.

Subsequent experiments were conducted, employing a thermal annealing method to fabricate gold nanodots. The thermal annealing process for creating gold nanodots involves heating a substrate, often quartz, coated with a thin film of gold to a high temperature in a controlled environment, such as an electric furnace. At high temperatures, the gold atoms within the thin film become highly mobile, facilitating their diffusion and rearrangement. Simultaneously, the high temperature induces thermal dewetting, causing the thin gold film to undergo surface restructuring due to surface energy reduction. This restructuring leads to the formation of discrete gold nanodots on the substrate. Over time, these nanodots grow as adjacent clusters merge, resulting in a uniform distribution of nanodots on the substrate surface. The annealing conditions are carefully selected to optimize the gold nanodots' size, density, and distribution, critical for various applications, including plasmonic biosensing. The acquired experimental results underwent rigorous analysis using data analysis software with image processing capabilities. The culmination of this investigative process involved meticulous scrutiny and synthesis of the experimental outcomes, culminating in identifying optimal factor levels conducive to the formation of gold nanoparticle dots. This thorough and iterative approach advances the understanding of gold nanodot formation. It lays the groundwork for refining and optimizing the nanofabrication process, contributing to enhancing biosensing technologies for applications in various scientific, medical, and industrial domains.

2.1 Design of Experiment

A 2^k full factorial design of an experiment is a type of experimental design widely used in statistical analysis and research. In this design, “k” factors are investigated, each at two levels. The term 2^k signifies the total number of experimental runs, where each factor is set at high and low levels. It is a systematic method for studying the joint effects of multiple factors on a response variable. The design systematically varies these factor levels to analyze their individual and interactive effects. The term "full factorial" implies that all possible combinations of factor levels are investigated. The total number of experimental runs is 2^k, making it efficient for studying multiple factors while minimizing the number of

experiments compared to a full enumeration. Statistical analysis, particularly Analysis of Variance (ANOVA) [25-27], is commonly applied to interpret the results and assess the significance of each factor and their interactions.

The 2^k full factorial designs method efficiently identifies significant factors in a statistical methodology, which helps optimize manufacturing processes. It is precious when producing gold nanodot arrays on a quartz substrate. By systematically varying process parameters, researchers can determine the most effective configuration for achieving desired properties in the nanodot arrays, improving precision and efficiency in the fabrication process.

2.1.1 Define the objectives.

This study focused on determining the diameter of gold nanodots on the substrate as its primary objective. The experiment aimed to provide valuable insights into the size characteristics of the fabricated nanostructures.

2.1.2 Identify the factors.

Identify critical process parameters influencing both the fabrication process and the properties of nanodot arrays. Key factors under consideration encompass the thickness of the gold thin film, annealing time, annealing temperature, and the surface treatment applied to the substrate, as shown in Table 1. A comprehensive analysis of these variables was imperative for optimizing the synthesis of gold nanodots.

TABLE 1. Levels of The Affecting Factors

No	Factor	Low	High
1	Gold Film Thickness	20 (nm)	30 (nm)
2	Annealing Time	20 (min)	30 (min)
3	Annealing Temperature	600 (°C)	700 (°C)
4	Surface Treatment	Without	Ethyl

TABLE 2. Design of The Experiment

Run	Gold Thickness (nm)	Annealing Time (min)	Annealing Temp (°C)	Surface Treatment
1	20	20	600	Without
2	30	20	600	Without
3	20	20	700	Without
4	30	20	700	Without
5	20	30	600	Without
6	30	30	600	Without
7	20	30	700	Without
8	30	30	700	Without

9	20	20	600	Ethyl
10	30	20	600	Ethyl
11	20	20	700	Ethyl
12	30	20	700	Ethyl
13	20	30	600	Ethyl
14	30	30	600	Ethyl
15	20	30	700	Ethyl
16	30	30	700	Ethyl

2.1.3 Determine the levels.

Understanding the influential factors governing gold nanodot formation is pivotal for the strategic design of subsequent experiments. This knowledge facilitates the refinement of experimental conditions for optimized outcomes in nanofabrication processes. The high-low level is shown in Table 1, followed by 2^k full factorial designs.

2.1.4 Design the experiment.

The experimental design employed the 2^4 Full Factorial Design method in this research. This experiment entailed having four controllable factors, with each element having two levels. The response variable was the average diameter of the gold nanodot on the quartz substrate. A total of 16 experiments were conducted, with each experiment replicated twice. Table 2 presents the comprehensive details of all experiments.

2.2 Research Processes

This research project aimed to develop a simplified and efficient method for fabricating gold nanoparticles using thermal annealing. When the gold film is heat-treated, it undergoes a process known as dewetting, which is the retraction of a thin film into discrete droplets or islands driven by surface energy reduction. The film breaks up into smaller clusters or nanodots.

As shown in Figure 1, initially (a), numerous voids manifested on the thin metal film. Subsequently (b), these voids expand and interconnect with adjacent voids. As this progression continues (c), the voids grow, leading to the partitioning of the metal film into islands. In the final stage (d), gold particles agglomerate on the substrate. This sequential transformation elucidates the dynamic process of thin gold film evolution under thermal annealing.

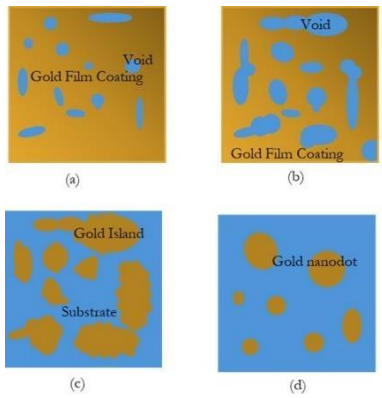

Figure 1. Thermal Annealing Method for The Gold Thin Film on A Quartz Substrate

The experimental procedure commenced with meticulously preparing the quartz glass surface through argon gas etching, effectively eliminating contaminants, followed by a thorough ultrasonic cleaning process. The substrates were stratified into two groups guided by the experimental design parameters. After the preparatory phase of the quartz substrate surface, the first group promptly underwent gold film coating. In contrast, the second group introduced an additional step, applying ethanal drops to the quartz substrate surface before the gold film coating, strategically reducing surface tension, as illustrated in Figures 2 and 3 sequentially.

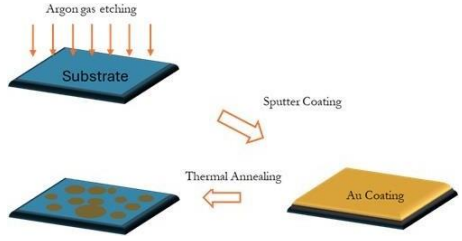

Figure 2. Experimental Group 1, Gold Nanodot Fabrication Process without Surface Treatment

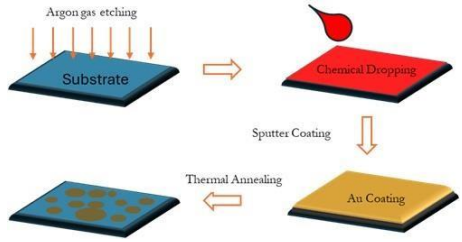

Figure 3. Experimental Group 2, Gold Nanodot Fabrication Process with Surface Treatment

Following these preparatory stages, a thin gold film was intricately coated onto the quartz substrate surface. The culmination of the process involved heating the thin gold film quartz substrate by the thermal annealing process to facilitate the fabrication of nanoparticles. This

method yielded 3D-gold nanodots characterized by diminutive diameters below 40 nanometers, as exemplified in Figure 4. Importantly, these nanodots were optimized for light absorption within the visible spectrum, rendering them highly suitable for applications in plasmonic sensing. This intricate and systematically devised methodology not only advances the fabrication of gold nanodots but also underscores their potential significance in enhancing optical properties, thereby contributing to the efficacy of plasmonic sensing technologies in various biosensing applications.

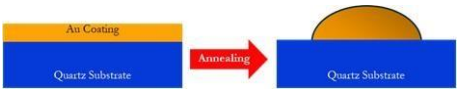

Figure 4. Gold Particles Agglomerate on The Substrate

2.2.1 Materials and Equipment

A gold (Au) sputtering target with a diameter of 50 mm was used in sputter deposition to deposit gold thin films onto a quartz substrate, Figure 5, a crystalline silicon dioxide material, is widely utilized in microelectronics and optics due to its exceptional thermal stability and transparency. Its unique properties make it an ideal choice for various research and industrial applications. The 1 mm thick Quartz substrate was cut into a size of 10×10 mm2 for this experiment.

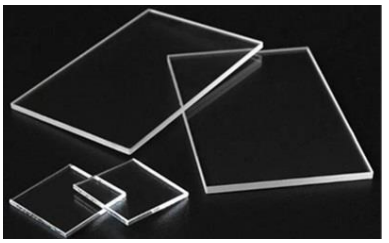

Figure 5. Quartz Substrate

A fume hood model FH-150-PP from Top Air System., Inc., Figure 6, is used in laboratories or areas involving chemical or hazardous substances. It features a front window or door that can be opened and closed, ensuring user safety from potential dangers released during operations inside the hood. It shields operators from chemical exposure or inhalation of Volatile Organic Compounds (VOCs) through direct contact or inhalation.

Figure 6. Fume Hood

In Figure 7, the ultrasonic cleaner machine model VGT-1613T from GT Sonic uses ultrasonic sound waves to clean various objects by removing stubborn dirt and contaminants.

Its operation involves generating ultrasonic waves to induce vibrations in the cleaning solution, creating bubbles and surface pressure to facilitate the removal of debris and deposits from target objects.

Figure 7. Ultrasonic Cleaner Model: VGT-1613T

In Figure 8, the DC sputter coating machine model MCM-200 from ISP Co., Ltd. is used in thin film deposition for various applications, including microscopy and material science. Sputter coating involves the removal of atoms from a target material (usually a metal) by bombarding it with ions. These ejected atoms then deposit onto a substrate, forming a thin film.

Figure 8. MCM-200 Ion Dc Sputter Coater

In Figure 9, an electric furnace model N 31/H from Nabertherm is a pivotal apparatus in materials science and metallurgy, providing controlled high-temperature environments for heat treatment and alloy production. Its utilization spans diverse industries, ensuring precision and efficiency in the fabrication and modification of materials, thus contributing significantly to scientific and industrial advancements.

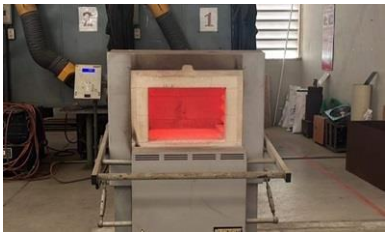

Figure 9. N 31/H Muffle Furnace

The Scanning Electron Microscope (SEM) model SU3000 from HITACHI as shown in Figure 10, is a potent tool for high-resolution imaging of nanoscale surfaces, finding extensive applications across diverse scientific and industrial domains. It serves as a crucial

instrument for meticulously scrutinizing the morphology and composition of specimens, contributing to advancements in research and industry.

Figure 10. Hitachi SU3000 Scanning Electron Microscope

2.2.2 Experimental Methods

Following the experimental procedures detailed in Figures 11 and 12, the initial step involved immersing a quartz substrate into a beaker containing 10 mL of acetone and then subjecting it to a thorough 15-minute ultrasonic cleaning process. Subsequently, the quartz substrate underwent a carefully regulated 2-minute self-drying phase within a fume hood. This meticulous procedure was strategically devised to eliminate residual fatty substances and contaminants from the substrate surface, creating an impeccably clean foundation. The primary objective was to ensure the substrate's pristine condition for subsequent phases in the experiment, safeguarding the integrity and reliability of the ensuing nanofabrication processes. This methodological precision underscores substrate preparation's critical role in the nanofabrication workflow's precision and reliability.

Applying an ethanol coating alleviated the quartz substrate's surface tension, as shown in Figure 13. This strategic measure enhanced and optimized the substrate's surface characteristics, a crucial step in ensuring the efficacy of subsequent nanofabrication processes.

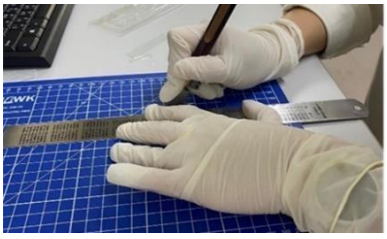

Figure 11. Quartz Substrate Preparation

Figure 12. Quartz Substrate Cleaning By The Ultrasonic Cleaner Machine

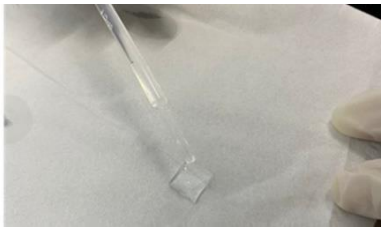

Figure 13. Chemical Dropping

After allowing the sample to dry thoroughly, the next step involves gold coating onto the quartz substrate. The sample was placed meticulously into the MCM-200 Ion Sputter Coater, as shown in Figure 14. Gold coatings of 20 and 30 nm thicknesses were sequentially applied according to the experimental design. For the 20 nm thickness, the electrical current was set at 0.5 mA for a coating duration of 300 seconds, and for the 30 nm thickness, the electrical current was set at 0.5 mA for a coating duration of 450 seconds.

In the final phase, the specimen underwent thermal annealing within an electric furnace at 600 and 700 degrees Celsius with annealing times of 20 and 30 minutes, respectively, to induce thermal annealing. This process facilitated the aggregation of metal particles on the substrate surface. Quartz substrates coated with thin gold films exhibited distinctive characteristics after thermal annealing.

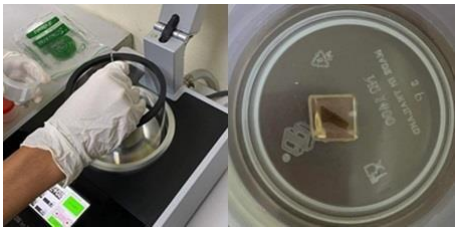

Figure 14. Gold Film Coating by The DC Sputter Coater Machine

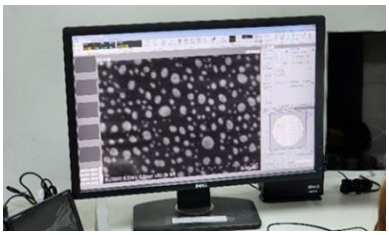

Figure 15. Scanning Electron Microscope (SEM) Software

The subsequent morphological transformations of the gold nanodot resulting from the thermal annealing were meticulously observed using Scanning Electron Microscopy (SEM), providing valuable insights into the structural evolution of the fabricated nanostructures.

2.3 Gold nanodot structure analysis

The thin gold film on the quartz substrate that had been heat-treated, induced dewetting will

turn into gold nanodot and look reddish pink as a result of the size-dependent surface plasmon resonance of the gold nanoparticles, and the thermal effects play a role in determining their size and arrangement., as shown in Figure 16.

The gold nanodot structure was analyzed using the image analysis software ImageJ, a Java-based image processing program. The analysis began with putting the specimen into the scanning electron microscope (SEM), as shown in Figure 10. Subsequently, areas suitable for analysis were identified and performed using SEM software, as shown in Figure 15. The analysis results yield the average dot diameter of the gold nanodot structure within that specific area, as shown in Figure 17.

Figure 16. Reddish-Pink Gold Nanodot

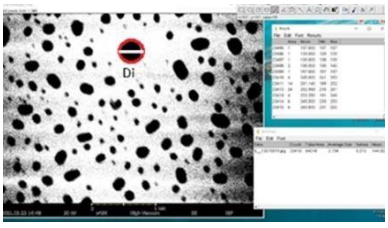

Figure 17. Image Analysis Process

3. RESULTS AND DISCUSSION

The 32 specimens from the experiments were meticulously examined using a scanning electron microscope. The analysis involved measuring the average nanodot diameter with Image processing software. This data identified the most suitable method for fabricating the gold nanodot, focusing on achieving the most minor average dot diameter. This analysis significantly influenced the precision of light absorption by the nanodot.

Subsequently, this information will be employed to advance and conduct experiments in future research, which involves creating an oxide layer (SiO_2) using the Plasma Enhanced Chemical Vapor Deposition (PECVD) technique, ultimately developing a multi-layer three-dimensional nanodot structure.

3.1 Experimental results

The experimental results of the gold nanodot fabrication method using the thermal annealing technique yielded measurements and analysis of the average gold nanodot diameter through

collaboration between the scanning electron microscope and the image analysis software. The results outcomes aligned closely with the objectives of this research work. Some notable examples are presented as follows.

Figure 18 scrutinized the gold nanodot structure resulting from a 20-nanometer thin film subjected to annealing at 600 degrees Celsius through scanning electron microscopy. The subsequent utilization of image processing software facilitated the determination of an average dot diameter, revealing a dimension of approximately 25 nanometers. This analysis contributes crucial insights into the structural characteristics achieved under specific fabrication conditions.

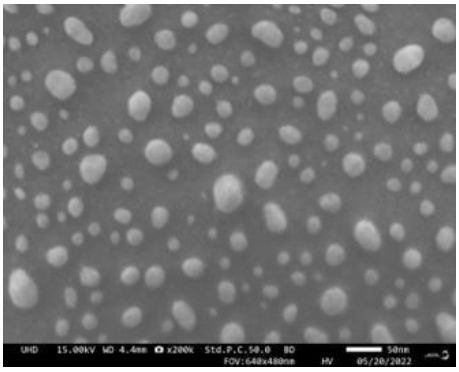

Figure 18. 20 (Nm) Thin Gold Film Analysis with Annealing At 600 (°C)

Figure 19 illustrates the gold nanodot structure derived from a 20-nanometer thin film following thermal annealing at 700 degrees Celsius. This process yielded an observed average dot diameter measuring approximately 32 nanometers. The image provides a visual representation of the impact of annealing conditions on the resultant size of the gold nanodots.

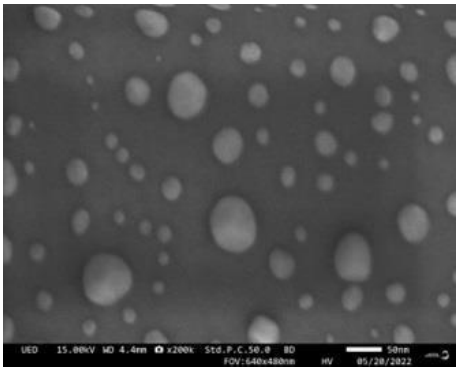

Figure 19. 20 (Nm) Thin Gold Film Analysis with Annealing At 700 (°C)

In Figure 20, the representation shifts to the gold nanodot structure from a 30-nanometer thin film. This film underwent annealing at 600 degrees Celsius, producing an average dot diameter of approximately 30 nanometers. These visualizations provide a comparative analysis of nanodot structures under distinct fabrication conditions, contributing valuable

insights into size variations based on film thickness and annealing temperature.

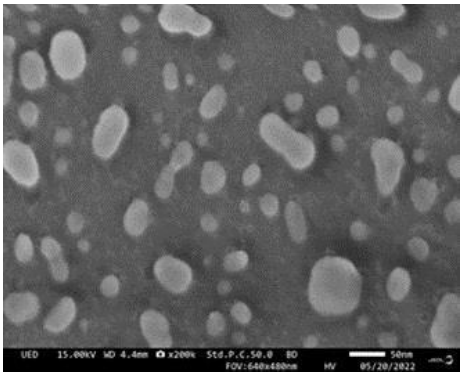

Figure 20. 30 (Nm) Thin Gold Film Analysis with Annealing At 600 (°C)

Figure 21 illustrates the gold nanodot structure derived from a 30-nanometer thin film following annealing at 700 degrees Celsius. This specific condition results in an average dot diameter of approximately 25 nanometers.

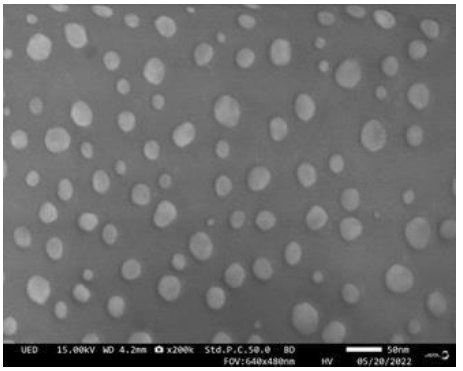

Figure 21. 30 (Nm) Thin Gold Film Analysis with Annealing At 700 (°C)

The image analysis results from each experimental trial, designed using the 2^4 Full Factorial, were evaluated. Four factors, Gold Film Thickness, Annealing Temp, Annealing Time, and Surface Treatment on the Substrate were selected as prototypes for biosensor development. Each factor had two levels, Low and High, and random experiments were conducted with two repetitions, totaling 32 trials. The designed experiments studied the factors and their levels, as shown in Table 1. The experimental outcomes, represented by the average diameter of the gold nanodot (in nanometers), are presented in Table 3. The results and variable data obtained from the experiments above were subjected to statistical analysis to confirm the reliability of the outcome data for further experiment summarization by Minitab version 21, Statistical data analysis, visualization, and quality improvement software.

3.2 Model adequacy checking

Adherence to specific assumptions is paramount in experimental design analysis with

multiple factors. The observed residuals must conform to a normal distribution, ensuring statistical robustness. Data independence and consistent variance values are also essential prerequisites. These stringent conditions guarantee the accuracy and reliability of the obtained results from variance analysis. Meeting these assumptions enables confidence in the applicability of the results for subsequent interpretation, providing a solid foundation for drawing meaningful insights from the experimental data and facilitating informed conclusions in the broader context of the research study.

3.2.1 Normal distribution analysis

Figure 22 displays a probability plot of residuals for the "smoothness" variable, illustrating a clear linear trend. This visually confirms the normal distribution of residual data, enhancing confidence in the statistical robustness of experimental results for smoothness.

3.2.2 Constant variance analysis

In Figure 23, the plot showcasing the relationship between residuals and the average diameter of gold nanodots on the quartz substrate (Versus Fits) elucidates a discernible trend marked by an independent distribution. This compelling evidence supports the assertion that data from this experimental set can be deemed reliable, bolstering the credibility and validity of the findings derived from the analysis.

3.2.3 Independently distributed analysis

Figure 24 depicts a graph juxtaposing the residual plot against the experimental order (Versus Order) for the response variable. The graph unveils a consistent trend, showcasing independent distribution for each experimental order. Notably, no discernible variability linked to factors or experimental order is evident. This robust homogeneity in the data reaffirms the reliability of the experimental set, establishing a solid foundation for accurate and meaningful interpretation of the findings within the scope of the research study.

3.2.4 Normality analysis

Figure 25 illustrates a histogram graph elucidating the variability in the average diameter of gold nanoparticles, displaying a natural distribution reminiscent of an inverted bell curve. Most of the data cluster near the center, presenting a well-balanced spread on both the left and right sides. This symmetrical distribution signifies a stable process, with minimal variability observed in the average central diameter of gold nanoparticles. The visual depiction of this balanced distribution pattern further reinforces the stability and consistency of the experimental process, contributing to the reliability and robustness of the obtained results.

Table 3. The Experiment Results

Run	Gold Thickness (nm)	Annealing Time (min)	Annealing Temp (°C)	Surface Treatment	Average Diameter (nm) Replicate 1	Replicate 2
1	20	20	600	Without	24.94263131	22.70797871
2	30	20	600	Without	35.77778639	41.5510474

3	20	20	700	Without	65.34492575	41.62282364
4	30	20	700	Without	29.70462952	29.33691655
5	20	30	600	Without	22.5764382	22.39523486
6	30	30	600	Without	30.49134409	44.17582246
7	20	30	700	Without	25.25488785	39.79375812
8	30	30	700	Without	31.26505274	35.59659522
9	20	20	600	Ethyl	27.14725836	27.14725836
10	30	20	600	Ethyl	23.86626987	20.51915861
11	20	20	700	Ethyl	19.45045763	25.04628409
12	30	20	700	Ethyl	26.01541437	36.52789881
13	20	30	600	Ethyl	28.70988271	20.51915861
14	30	30	600	Ethyl	35.67856677	37.20397343
15	20	30	700	Ethyl	26.90112933	24.84676175
16	30	30	700	Ethyl	17.38172462	26.35567133

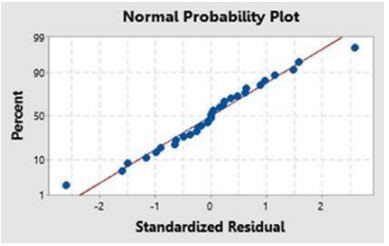

Figure 22. Normal Probability Plot

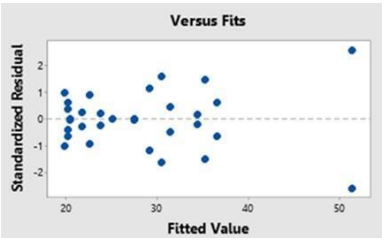

Figure 23. Constant Variance

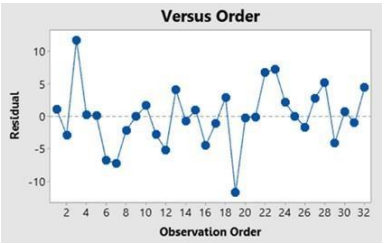

Figure 24. Independently Distributed

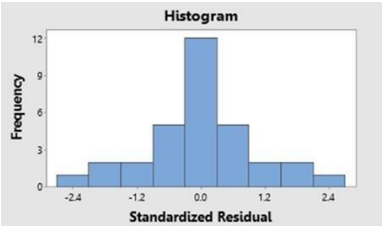

Figure 25. Normality Histogram

3.3 Factor Analysis

The ANOVA is a commonly used statistical tool for studying and estimating the factors influencing a process. The F-statistic, prominent in statistical analysis in conjunction with ANOVA, assesses significant differences among means of multiple groups. It compares variation between and within groups, allowing for hypothesis testing. A large F-value implies differences unlikely due to chance, rejecting the null hypothesis and indicating significant group mean differences. Utilizing the F-Test table involves calculating the F-statistic, determining degrees of freedom, and identifying the significance level (α), typically set at 0.05. Locate the critical F-value in the table using α and degrees of freedom. If the calculated F exceeds this value, reject the null hypothesis, signifying significant group mean differences. Conversely, if the calculated F is less, it fails to reject the null hypothesis, indicating no significant differences among group means. This experiment involved the measurement of the average diameter of gold nanostructures, employed as the response variable for subsequent variance analysis. A confidence level of 95% was established, with a significance level (α) of 0.05, aiming to discern influential factors in the experiment. Utilizing the Minitab program, Table 4 presents the comprehensive analysis results. This statistical approach, executed at a rigorous confidence level, enhances the reliability of the findings, facilitating a nuanced understanding of the factors shaping gold nanostructure diameter and their impact on the experimental outcomes.

The extensive analysis presented in Table 4 underscores the significant impact of various factors on the response variable. Notably, the significant effect of the gold nanodot aggregation comes from Factor D: Surface treatment on Substrate, evidenced by an F-value test of 10.72. This test value surpassed the critical F-value (FC) from the F-Test table, set at 4.494, signifying the pronounced significance of Factor D compared to the variance attributed to experimental error values. In contrast, Factor A: Gold Film Thickness registered a test value of 1.03, Factor B: Annealing Temp recorded 0.93, and Factor C: Annealing Time yielded 0.57. These values fell below the critical F-value, indicating their negligible

influence on the average gold nanodot diameter, substantiating the pivotal role of Factor D in shaping the experimental outcomes.

Includes the interaction between factors that predominantly influenced the average gold nanodot diameter compared to all other factors and their interactions at various levels, namely:

The interaction between two factors: A and B.

The interaction between three factors: A, B, and D.

The interaction from all factors: A, B, C, and D.

Table 4. Analysis of Variance

Source	Degree of Freedom	Sum of Square	Mean Square	F-Value	P-Value
Model	15	2154.41	143.627	3.47	0.009
A	1	42.88	42.876	1.03	0.324
B	1	38.36	38.358	0.93	0.35
C	1	23.74	23.741	0.57	0.46
D	1	444.18	444.176	10.72	0.005
AB	1	372.61	372.613	8.99	0.008
AC	1	102.47	102.467	2.47	0.135
AD	1	3.46	3.458	0.08	0.776
BC	1	126.98	126.981	3.06	0.099
BD	1	160.06	160.06	3.86	0.067
CD	1	82.29	82.293	1.99	0.178
ABC	1	3.06	3.061	0.07	0.789
ABD	1	323.72	323.715	7.81	0.013
ACD	1	55.79	55.786	1.35	0.263
BCD	1	1.21	1.212	0.03	0.866
ABCD	1	373.61	373.612	9.02	0.008
Error	16	662.92	41.432		
Total	31	2817.33			

The main effect plot using the ANOVA general linear model also shows that factor D is significant compared to A, B, and C, as shown in Figure 26; it serves as a graphical representation of the response variable, the diameter of gold nanoparticles on the quartz substrate across different levels of the experimental factors.

The graphical depiction in Figure 27 offers the interaction of factors influencing the formation of gold nanoparticles. The intersection points of graph lines signify factors significantly impacting the nanostructure fabrication process, while parallel lines indicate lesser significance.

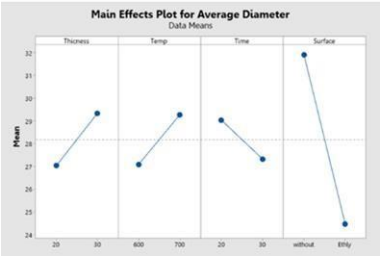

Figure 26. Main Effects Plot

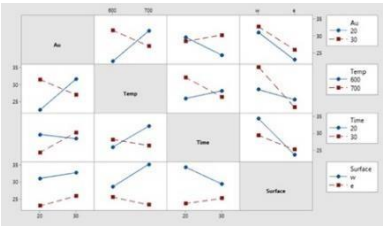

Figure 27. Interaction Plot

In the pursuit of optimization, the Minitab software conducted a comprehensive analysis to discern the optimal factor and its associated levels. This approach was employed to identify the specific characteristics and levels significantly influencing the diameter of gold nanoparticles fabricated on the quartz substrate. Optimal levels for the gold nanodot fabrication process were discerned through meticulous primary and interaction effects analysis. Namely, Factor A exhibited heightened efficacy at a high level (Gold Film Thickness of 30 nanometers), Factor B showcased optimal performance at a high level (annealing temperature of 700 degrees Celsius), Factor C demonstrated efficiency at a high level (annealing time of 30 minutes), and Factor D displayed effectiveness at a high level (with chemical treatment on the quartz substrate). The ensuing average diameter for these identified optimal factor levels measured 21.8687 nanometers, underscoring the significance of these specific conditions in achieving precise control over gold nanoparticle characteristics during the fabrication process.

3.4 Experimental Confirmation

To verify the experiment results, this research conducted experiments to confirm whether the appropriate level of factors from the experiment results would affect the average diameter of gold nanoparticles as desired. By setting various factor values based on the experimental

results, which include:

Factor A: Gold Film Thickness of 30 nanometers.

Factor B: The annealing temperature of 700 degrees Celsius.

Factor C: The annealing time of 30 minutes.

Factor D: With chemical treatment on the quartz substrate.

Table 5. Experiment Confirmation

Run	Gold Thickness (nm)	Annealing Time (min)	Annealing Temp (°C)	Surface Treatment	Average Diameter (nm)
1	30	30	700	Ethyl	26.9855
2	30	30	700	Ethyl	20.7238
3	30	30	700	Ethyl	24.6671
4	30	30	700	Ethyl	22.4241
5	30	30	700	Ethyl	20.1879
6	30	30	700	Ethyl	20.4460

From Table 5, this study conducted tests to confirm whether the average diameter of gold nanodots from the sample group of 6 experiments was equal to the average diameter obtained from the Design of Experimental results, which is 21.8687 nanometers, at a significance level of 0.05. The calculated P-value of 0.557 exceeded 0.05. Therefore, it was concluded that the experiments had an average diameter of gold nanoparticles equal to 21.8687 nanometers, with a mean of 22.57 nanometers and a confidence interval of 19.70 to 25.45. Consequently, the factor level values obtained from the Design of Experimental can be used to fabricate the gold nanodot.

3.5 Discussion

The thermal annealing process at a temperature of 700 degrees Celsius for 30 minutes in an electric furnace is a critical step in the fabrication process of gold nanodots on the quartz substrate. This specific temperature and duration have been chosen for several reasons based on their influence on the 30 nanometers thin gold film on a quartz substrate treated with ethyl.

In the aggregation of gold nanostructure at elevated temperatures, such as 700 degrees Celsius, that facilitates the diffusion and rearrangement of gold atoms on the thin film, the gold atoms become highly mobile. Simultaneously, the high temperature promotes the thermal dewetting process, where the thin gold film undergoes surface restructuring due to surface energy reduction. This restructuring results in the formation of discrete gold nanodots on the quartz substrate. 30-minute duration allows for sufficient time for the gold atoms to migrate and self-assemble into nanodots. As the annealing time progresses, these clusters merge and grow, forming distinct gold nanodots.

The chosen temperature and duration result in an optimized size and distribution of gold nanodots. The specific parameters depend on factors like the initial thickness of the gold film at 30 nanometers and the rate of diffusion, which is caused by the treatment on the quartz substrate with ethyl, which likely serves as a surface modification to enhance the nucleation sites for gold nanodot formation. It can influence the wetting properties, adhesion, and interaction between the gold film and the substrate.

The optimum condition for gold nanodot aggregation, as identified in this study, involves several key parameters: a gold film thickness of 30 nm, an annealing temperature of 700°C, an annealing time of 30 minutes, and ethanol surface treatment on the quartz substrate. The mechanism behind these conditions can be understood through various physical and chemical processes during nanofabrication. The thickness of the gold film determines the amount of gold available for nanodot formation. However, a thicker film may lead to excessive aggregation or irregularities in nanodot size, while a thinner film may result in insufficient material for aggregation. Therefore, the 30 nm thickness likely provides an optimal balance for controlled nanodot formation. Moreover, thermal annealing plays a crucial role in promoting the diffusion and aggregation of gold atoms into nanodots. At elevated temperatures, the mobility of gold atoms increases, allowing them to migrate and form clusters. The chosen temperature of 700°C is likely within a range where the diffusion of gold atoms is sufficiently rapid without causing excessive surface roughness or degradation of the substrate. The 30-minute annealing time allows for adequate diffusion and aggregation while minimizing the risk of overgrowth or coalescence of nanodots. Furthermore, Ethanol treatment likely serves to clean the quartz substrate surface and modify its properties to facilitate the nucleation and adhesion of gold nanoparticles. Ethanol treatment may remove surface contaminants or oxides, promoting better adhesion and nucleation of gold atoms during annealing. Additionally, it may introduce functional groups or defects on the substrate surface that enhance the nucleation sites for gold nanodots.

The combined effect of these optimal conditions likely promotes uniform nucleation and controlled growth of gold nanodots on the quartz substrate. The thickness of the gold film, along with the annealing temperature and time, influences the diffusion kinetics and aggregation behavior of gold atoms, leading to the formation of nanodots with the desired diameter. The ethanol surface treatment further enhances the nucleation and adhesion of gold nanoparticles, contributing to the uniformity and stability of the nanodot arrays. In summary, the optimal conditions identified in this study represent a delicate balance of factors that control the nucleation, growth, and aggregation of gold nanodots, ultimately leading to the desired diameter and morphology of the nanodot arrays for plasmonic biosensing applications.

In summary, the annealing process at 700 degrees Celsius for 30 minutes promotes the diffusion and rearrangement of gold atoms on the thin film, leading to the optimum aggregation of gold nanodots on the quartz substrate. The ethyl treatment on the quartz substrate enhances the nucleation sites, contributing to the nanodot's controlled growth and distribution. After treating the substrates chemically, Ethyl molecules adhered to the substrate surface upon dropping. Even after the Ethyl drop had dried, these molecules persisted on the substrate. Consequently, the gold film coated the layer of molecules. Upon annealing this substrate, the gold thin film readily agglomerated onto the gold nano-island

array of the substrate, resulting in a smaller dot diameter than a substrate without Ethyl treatment. The specific parameters are determined through experimentation and optimization based on the desired characteristics of the gold nanodot array.

In a study focusing on the thermal annealing process to fabricate gold nanodots on the quartz glass substrate, potential sources of error can arise from various aspects of the experimental setup, execution, and measurement. The variations in experimental conditions are possible sources of error, such as temperature gradients within the annealing furnace, humidity, and atmospheric pressure, which can affect the reproducibility of the nanodots on the substrate. Furthermore, the external contaminants or impurities in the materials used for fabrication or during the experimental process can influence the formation and characteristics of the gold nanodots.

Thermal annealing is a commonly used technique to fabricate gold nanostructures by heating and cooling gold-containing materials. At the same time, thermal annealing has certain limitations when fabricating gold nanostructures. For example, during thermal annealing, there is a risk of surface contamination, which can affect the properties of the gold nanostructures. Contaminants from the atmosphere or the substrate material may absorb onto the surface of the nanostructures, altering their chemical composition or surface properties. Controlling the potential for surface contamination during the thermal annealing process is aimed at minimizing the introduction of impurities and maintaining a clean environment. Therefore, monitoring the annealing process in real-time using techniques such as hot stage characterized the dynamic observation of scanning electron microscopy to detect any changes in the surface chemistry or morphology of the nanostructures. This allows for immediate adjustments to the process parameters if contamination is observed.

Gold nanodots fabricated via thermal annealing can exhibit enhanced sensitivity in biosensing applications compared to larger gold nanoparticles. The small size of nanodots results in a higher surface area-to-volume ratio, allowing for increased interactions with target biomolecules. This enhanced surface area can lead to improved sensitivity in detecting low concentrations of analytes, such as proteins, nucleic acids, or small molecules.

For future research, avenues for further optimizing the fabrication process will be explored. However, additional parameters such as the type of noble materials and the type of chemical treatment could be investigated to improve this nanofabrication method's efficiency, reproducibility, or scalability.

4. CONCLUSION

The primary objective of this research was to discern optimal parameter values for fabricating gold nanodots on a quartz substrate through the thermal annealing process. Employing a 2^k factorial design in the experimental framework, the investigation aimed to identify suitable levels for each factor to enhance precision and control in the nanofabrication process. The experimental design adopted a 2^4-full factorial approach, selecting four factors, each manipulated at two levels, as detailed in Table 1. With 32 trials conducted in a replicated manner, including two repetitions, the experimental conditions were systematically randomized to ensure comprehensive coverage and facilitate a robust

determination of optimal factors for the thermal annealing-based fabrication of gold nanodots on a quartz substrate.

This research's focal examination point was the response variable, the average diameter of the resulting gold nanodots. The ensuing analysis brought forth pivotal insights, unveiling the prominence of Factors A, B, C, and D as substantial influencers on the response variable, attaining statistical significance at a robust 95% confidence level.

From the summary of the experimental results, Factor A, the thickness level of gold coating on the quartz substrate, had two levels, 20 and 30 nanometers. The analysis indicates that a thickness of 30 nanometers was the most suitable for serving as a template. Regarding Factor B, the optimal annealing temperature ensures proper gold dot aggregation. An annealing temperature of 700 degrees Celsius promotes complete nanodot formation and uniform distribution across the quartz substrate, facilitating analysis. Factor C, annealing time, significantly influenced the process. A suitable annealing time was 30 minutes, creating well-structured and uniformly distributed gold nanodots. Factor D, the chemical used during annealing, had the maximum impact on nanostructure formation. The chemical aimed to reduce surface tension, and since the quartz substrate had a coated film, chemical dripping was necessary for the nanodot fabrication process.

The carefully chosen thermal annealing conditions of 700 degrees Celsius for 30 minutes facilitate controlled aggregation, coalescence, and surface restructuring of the 30 nanometers thin gold film. This results in the optimal aggregation of gold nanodots on the quartz substrate, ensuring the desired size, stability, and optical properties. The insights gained from identifying these influential factors contribute to refining and optimizing the nanofabrication process, enhancing precision in controlling the gold nanostructure diameter on a quartz substrate. The robustness of these findings is affirmed by the systematic exploration through a 2^k factorial design, randomization, and replication, providing valuable guidance for achieving specific characteristics in gold nanodots and advancing nanotechnology applications.

ACKNOWLEDGEMENT

The authors would like to acknowledge Dr. W. Rattanasakulthong and the Department of Physics, Kasetsart University, for their support and encouragement.

The authors would like to acknowledge the facility support from the School of Engineering at the University of Phayao.

*Corresponding Author: Assistant Professor, School of Engineering, University of Phayao, Thailand. E-Mail: potejanasak.po@up.ac.th

References

1. Guo, L., Jackman, J. A., Yang, H.-H., Chen, P., Cho, N.-J., & Kim, D.-H. (2015). Strategies for enhancing the sensitivity of plasmonic nanosensors. Nano Today, 10(2), 213-239. https://doi.org/https://doi.org/10.1016/j.nantod.2015.02.007
2. Thi, M. L. N., Pham, V. T., Bui, Q. B., Ai-Le, P. H., & Nhac-Vu, H. T. (2020). Novel nanohybrid of blackberry-like gold structures deposited graphene as a free-standing sensor for effective hydrogen peroxide detection. Journal of Solid State Chemistry, 286, 121299.

https://doi.org/https://doi.org/10.1016/j.jssc.2020.121299
3. Li, W., Zhang, L., Zhou, J., & Wu, H. (2015). Well-designed metal nanostructured arrays for label-free plasmonic biosensing [10.1039/C5TC00553A]. Journal of Materials Chemistry C, 3(25), 6479-6492. https://doi.org/10.1039/C5TC00553A
4. Hwang, C., Ahn, M.-S., Lee, Y., Chung, T., & Jeong, K.-H. (2019). Ag/Au Alloyed Nanoislands for Wafer-Level Plasmonic Color Filter Arrays. Scientific Reports, 9. https://doi.org/10.1038/s41598-019-45689-9
5. Ahn, H., Song, H., Choi, J.-R., & Kim, K. (2017). A Localized Surface Plasmon Resonance Sensor Using Double-Metal-Complex Nanostructures and a Review of Recent Approaches. Sensors, 18, 98. https://doi.org/10.3390/s18010098
6. Takemura, K. (2021). Surface Plasmon Resonance (SPR)- and Localized SPR (LSPR)-Based Virus Sensing Systems: Optical Vibration of Nano- and Micro-Metallic Materials for the Development of Next-Generation Virus Detection Technology. Biosensors, 11, 250. https://doi.org/10.3390/bios11080250
7. Gutierrez-Rivera, L., Peters, R., Dew, S., & Stepanova, M. (2013). Application of EBL fabricated nanostructured substrates for surface enhanced Raman spectroscopy detection of protein A in aqueous solution. Journal of Vacuum Science & Technology B: Microelectronics and Nanometer Structures, 31, 06F901-906F901. https://doi.org/10.1116/1.4821800
8. Agrawal, A., Majdi, J., Clouse, K., & Stantchev, T. (2018). Electron-Beam-Lithographed Nanostructures as Reference Materials for Label-Free Scattered-Light Biosensing of Single Filoviruses. Sensors, 18, 1670. https://doi.org/10.3390/s18061670
9. Yoon, G., Kim, I., So, S., Mun, J., Kim, M., & Rho, J. (2017). Fabrication of three-dimensional suspended, interlayered and hierarchical nanostructures by accuracy-improved electron beam lithography overlay. Scientific Reports, 7. https://doi.org/10.1038/s41598-017-06833-5
10. Friedensen, S., Mlack, J., & Drndić, M. (2017). Materials analysis and focused ion beam nanofabrication of topological insulator Bi2Se3. Scientific Reports, 7. https://doi.org/10.1038/s41598-017-13863-6
11. Liu, Y., King, H., van Huis, M., Drury, M., & Plümper, O. (2016). Nano-Tomography of Porous Geological Materials Using Focused Ion Beam-Scanning Electron Microscopy. Minerals, 6, 104. https://doi.org/10.3390/min6040104
12. Carvalho-de-Souza, João L., Treger, Jeremy S., Dang, B., Kent, Stephen B. H., Pepperberg, David R., & Bezanilla, F. (2015). Photosensitivity of Neurons Enabled by Cell-Targeted Gold Nanoparticles. Neuron, 86(1), 207-217. https://doi.org/https://doi.org/10.1016/j.neuron.2015.02.033
13. Phuc, T. D., Yoshino, M., Yamanaka, A., & Yamamoto, T. (2013). Fabrication of Gold Nanodot Array on Plastic Films for Bio-sensing Applications. Procedia CIRP, 5, 47-52. https://doi.org/https://doi.org/10.1016/j.procir.2013.01.009
14. Axelevitch, A., Apter, B., & Golan, G. (2013). Simulation and experimental investigation of optical transparency in gold island films. Optics express, 21, 4126-4138. https://doi.org/10.1364/OE.21.004126
15. Yoshino, Kubota, Nakagawa, & Terano. (2019). Efficient Fabrication Process of Ordered Metal Nanodot Arrays for Infrared Plasmonic Sensor. Micromachines, 10, 385. https://doi.org/10.3390/mi10060385
16. Li, Z., Yoshino, M., & Yamanaka, A. (2014). Regularly-formed three-dimensional gold nanodot array with controllable optical properties. Journal of Micromechanics and Microengineering, 24(4), 045011. https://doi.org/10.1088/0960-1317/24/4/045011
17. Phuc, T. D., Yoshino, M., Yamanaka, A., & Yamamoto, T. (2014). Effects of Morphology of Nanodots on Localized Surface Plasmon Resonance Property. International Journal of Automation Technology, 8(1), 74-82. https://doi.org/10.20965/ijat.2014.p0074
18. Kanmaz, İ., & Üzüm, A. (2021). Silicon dioxide thin films prepared by spin coating for the

application of solar cells. International Advanced Researches and Engineering Journal, 05, 14-018. https://doi.org/10.35860/iarej.784328

19. Potejanasak, P., & Seemuang, N. (2019). Fabrication of Metallic Nano Pillar Arrays on Substrate by Sputter Coating and Direct Imprinting Processes. Applied Science and Engineering Progress. https://doi.org/10.14416/j.asep.2019.09.001
20. Quan, J., Zhang, J., Qi, X., Li, J., Wang, N., & Zhu, Y. (2017). A study on the correlation between the dewetting temperature of Ag film and SERS intensity. Scientific Reports, 7. https://doi.org/10.1038/s41598-017-15372-y
21. Huang, Q.-A., Jiang, W., & Yang, J. (2019). An Efficient and Unconditionally Energy Stable Scheme for Simulating Solid-State Dewetting of Thin Films with Isotropic Surface Energy. Communications in Computational Physics, 26, 1444-1470. https://doi.org/10.4208/cicp 2019.js60.07
22. Zhou, L., Poggesi, S., Giuliocesare, C. B., Mittapalli, R., Adam, P.-M., Manzano, M., & Ionescu, R. (2019). Robust SERS Platforms Based on Annealed Gold Nanostructures Formed on Ultrafine Glass Substrates for Various (Bio)Applications. Biosensors, 9, 53. https://doi.org/10.3390/bios9020053
23. Li, Z., Yoshino, M., & Yamanaka, A. (2013). Optical Properties of Multilayer Ordered Gold Nanodot Array Fabricated by a Thermal Dewetting Method. Procedia CIRP, 5, 42–46. https://doi.org/10.1016/j.procir.2013.01.008
24. Ramli, A. B., Izamshah, R., & Razak@ali, L. (2019). Application of Full Factorial Analysis Design For Determining Surface Roughness Model In End Milling of Hardened Steel Material Using Solid Carbide Niti Co 30 Standard End Mill. Proceeding of the Malaysia TVET on Research via Exposure 2019, Politeknik Muadzam Shah, Pahang.
25. Montgomery, D., & St, C. (2022). Design and Analysis of Experiments. (9th ed.). John Wiley & Sons, Inc.
26. Rajalakshmi, N., Guruviah, V., & Dhathathreyan, K. S. (2009). Sensitivity Analysis of a 2.5 kW Proton Exchange Membrane Fuel Cell Stack by Statistical Method. Journal of Fuel Cell Science and Technology - J FUEL CELL SCI TECHNOL, 6. https://doi.org/10.1115/1.2971053
27. Gopalsamy, B., Mondal, B., & Ghosh, S. (2009). Taguchi method and ANOVA: An Approach for process parameters optimisation of Hard Machining while machining hardened steel. Journal of scientific and industrial research, 68, 686-695.